Contents lists available at ScienceDirect

Algal Research

Salinity stress provokes diverse physiological responses of eukaryotic unicellular microalgae

Attila Farkas [a], Bernadett Pap [a], Ottó Zsíros [a], Roland Patai [b], Prateek Shetty [a], Győző Garab [a,c], Tibor Bíró [d], Vince Ördög [e,f], Gergely Maróti [a,d,g,*]

[a] Institute of Plant Biology, Biological Research Centre, Szeged, Hungary
[b] Institute of Biophysics, Biological Research Centre, Szeged, Hungary
[c] Department of Physics, Faculty of Science, University of Ostrava, Ostrava, Czech Republic
[d] Faculty of Water Sciences, National University of Public Service, Baja, Hungary
[e] Department of Plant Sciences, Albert Kázmér Mosonmagyaróvár Faculty, Széchenyi István University, Győr, Hungary
[f] Research Centre for Plant Growth and Development, School of Life Sciences, University of KwaZulu-Natal, Campus Pietermaritzburg Campus, Scottsville, Pietermaritzburg, South Africa
[g] Seqomics Biotechnology Ltd., Mórahalom, Hungary

ARTICLE INFO

ABSTRACT

Highly saline conditions represent a strong challenge for most microorganisms in freshwater ecosystems. Eukaryotic freshwater green algae from the Chlorophyta clade were investigated for their ability to survive in and adapt to increased salt concentration in the growth medium. Striking differences were detected between the responses of the various algae species to the elevated salt concentrations. The investigated *Chlamydomonas reinhardtii* cc124 and *Coelastrella* sp. MACC-549 algae showed a moderate resistance to increased salt concentration, while *Chlorella* sp. MACC-360 exhibited high salt tolerance, showed unaltered growth characteristics and photosynthetic efficiency compared to the saline-free control conditions even at 600 mM NaCl concentration. Diverse physiological responses to elevated salt concentrations were described for the tested algae including variations in their growth capacity, characteristic morphological changes, alterations in the structure and function of the photosynthetic machinery and differences in the production of reactive oxygen species. Special alterations were identified in the lipid and exopolysaccharide production patterns of the tested algal strains in response to high salinity. As a conclusion *Chlorella* sp. MACC-360 algae showed outstanding salt tolerance features. Together with the concomitant lipid-producing phenotype under highly saline conditions this unicellular green alga is a promising candidate for biotechnological applications.

1. Introduction

Microalgae are important primary producers [1] and play a pivotal role in natural ecosystems by modulating global carbon cycling. Algae are also industrially relevant organisms in bio-based industries ranging from wastewater treatment through feed for aquaculture to biofuels [2]. Both prokaryotic and eukaryotic algae are ubiquitous in most environments including extreme conditions like salt lakes and soda pans. Changing salinity of the growth medium is a great challenge for microalgae mass cultivation in open raceway ponds [3]. Robust and halotolerant species can survive and grow under these conditions [4,5].

Selection and investigation of eukaryotic algae possessing great plasticity and adaptability to most abiotic stresses including high salinity is an increasing demand. Certain algae species can grow in both fresh and saline water, however, most of the freshwater and soil eukaryotic algae are sensitive to high salt concentration. Algae apply several different survival strategies in response to stress. It is important to distinguish between short-term acclimation responses and long-term adaptation mechanisms. Short-term acclimation refers to algal activity in response to periodic variations in osmotic concentration lasting a few days, whereas long-term adaptation refers to algal selection in response to persistent change in osmotic concentration [6,7]. Short-term responses require drastic changes in morphology and rapid actions in modifying osmolyte concentrations, while long-term adaptation mostly represents accumulation of advantageous mutations [8]. The short-term acclimation strategies largely depend on the strength and type of the

---

specific abiotic stress as well as on the duration of exposure to the stress.

A common survival strategy of the planktonic unicellular organisms is the rapid formation of multicellular structures, mainly biofilms. Biofilms provide physical defense to most of the cells by simply separating a large fraction of the cells from the stressor and through a secreted exopolysaccharide (EPS) matrix. Unicellular green algae also apply this strategy [9]. The most information on salt-mediated short-term algal responses are available for the model green algae *Chlamydomonas reinhardtii*. The first stress response of *C. reinhardtii* is the loss of flagella [10]. Palmelloid formation is also a highly characteristic *Chlamydomonas* response to various abiotic stresses. Under highly saline conditions, the planktonic algal cells transform into palmelloid structure, where the cells remain in close vicinity to each other embedded in exopolysaccharides and surrounded by a common membrane [11,12]. Thus, EPS secretion is another common strategy of *C. reinhardtii* cells to defend themselves against the osmotic stress. However, palmelloidy is only a temporary stage, the colonial-like structure quickly disassemble when stress-free conditions are restored [13].

The short-term stress responses are diverse across various green algae species. The accumulation of lipid droplets was observed in the alga *Parachlorella kessleri* grown under saline stress conditions [14]. The lipid droplets likely mediate the accumulation of compatible solutes and antioxidants, which are important tools in coping with high salt concentration. Mannitol is another compatible solute with multiple functions including osmoregulation, storage, regeneration of reducing power and scavenging of active oxygen species as demonstrated mostly in red algae [15]. High salinity stress can be used as an inducer of increased production of valuable algal metabolites, like carotenoid astaxanthin in *Haematococcus pluvialis* [16]. Salt stress is an efficient enhancer of the lipid content and lipid yield in the cells of *Chlorella protothecoides* [17].

The objective of this study was to investigate the effects of high salinity on three species of unicellular green algae from distinct genera of Chlorophyta: *Chlamydomonas reinhardtii* cc124, *Coelastrella* sp. MACC-549 and *Chlorella* sp. MACC-360. These strains were chosen due to their distinct growth rates and contrasting responses to salt stress. This selection made possible the comparison of short-term responses of various Chlorophyta algal species to saline stress.

2. Materials and methods

2.1. Strains and growth conditions

Coelastrella sp. MACC-549 and *Chlorella* sp. MACC-360 algal strains were selected from the Mosonmagyaróvár Algal Culture Collection (MACC). *Chlamydomonas reinhardtii* cc124 was obtained from the Institute of Plant Biology, Biological Research Centre of the ELKH. Axenic algal strains were grown and maintained on TP (Tris-Phosphate) medium supplemented with rifampicin (50 μg/mL). The TP medium is a modified TAP (Tris-Acetate-Phosphate) medium where acetic acid is replaced by HCl to adjust pH 7 [18]. The algal strains were incubated on TP plates under continuous 50 μmol photons m^{-2} s^{-1} light intensity at 25 °C. Algae used for salt stress experiments were inoculated from TP plates into liquid TAP medium. Algal liquid cultures in TAP medium were incubated in 100 mL Erlenmeyer flasks under 50 μmol photons m^{-2} s^{-1} light intensity using a light/dark cycle of 16:8 h at 25 °C and shaken at 180 rpm. Algae stock solutions were generated using fresh cultures by centrifugation and re-suspending the cells in fresh TAP medium. The final optical densities of the algal cells to be challenged by various concentrations (see details in the Results section) of salt (NaCl) were set to 1 (OD_{750}) for each tested algal strain. Semi-high throughput cultivation method using 24-well, flat-bottom microtiter plates was applied for the determination of salt tolerance of the three algal strains (1.5 mL algal cultures were cultivated in each well). All experiments aiming the investigation of salt stress on algal growth were performed at least in triplicates.

2.2. Microscopy analyses

Microscopic investigations of control and salt-stressed algal cells and cultures were performed using various microscopy techniques. An Olympus Confocal Laser Scanning Microscope (CLSM, Olympus Fluoview FV-300, Olympus Optical Co., Ltd., Tokyo, Japan) was used for the fluorescence identification of secreted extracellular metabolites in this study. 50 μL cultures were taken to Eppendorf tubes and stained with 10 μg/μL Calcfluor White (CFW) and Concanavalin A (Con A), respectively [19–21]. After 30 min incubation in dark, the samples (8 μL) were spotted on microscope slides and covered with 2 % (w/v) agar slice and observed with CLSM using a 63× magnification objective. Sequential scanning was used to avoid crosstalk of the fluorescent dyes and chlorophyll autofluorescence. To 50 μL microalgal cultures, 0.25 μL of 4 mM BODIPY dye was added to stain the lipid droplets [22] and then cells were observed under an Olympus Confocal Laser Scanning Microscope (CLSM, Olympus Fluoview FV-300, Olympus Optical Co., Ltd., Tokyo, Japan). For BODIPY, the excitation range was selected between 500 nm to 515 nm (excitation, 500 nm; emission, 515 nm).

Scanning and transmission electron microscopes were utilized for the detailed structural investigation of the algal cells. For scanning electron microscopy (SEM) algal cells were fixed overnight with 2.5 % (v/v) glutaraldehyde and 0.05 M cacodylate (pH 7.2) in phosphate buffered saline (PBS) pH 7.4. 5 μL samples were spotted on a silicon disk coated with 0.01 % Poly-ʟ-Lysine. The discs were washed twice with PBS and dehydrated overnight with a graded ethanol series (30 %, 50 %, 70 %, 80 %, and 100 % ethanol). The samples were dried with a critical point dryer, followed by 12 nm gold coating, and observed under a JEOL JSM-7100F/LV field-emission scanning electron microscope.

For transmission electron microscopy (TEM) algae samples were fixed overnight in Karnovsky solution containing 2 % paraformaldehyde (Sigma; St. Louis, MO, United States) and 2.5 % glutaraldehyde (Polysciences; Warrington PA, United States) in PBS at 4 °C. After the fixation, samples were rinsed in distilled water (pH 7.4) for 10 min followed by a 2-hour long incubation in 2 % osmium tetroxide (OsO_4) solution (dissolved in distilled water, pH 7.4). Afterwards, samples were briefly rinsed in distilled water for 10 min, then dehydrated in a graded series of ethanol (increased from 50 % to 100 %) for 30 min at each concentration and finally the samples were proceeded through propylene oxide. All dehydrated and osmificated samples were embedded in an epoxy-based resin (Durcupan ACM; Sigma), then polymerized at 56 °C for 48 h. From the polymerized resin blocks, 50 nm ultrathin sections were cut on an Ultracut UCT ultramicrotome (Leica; Wetzlar, Germany) and samples were mounted on single-hole formvar-coated copper grids (Electron Microscopy Sciences; Hatfield, PA, United States). For a better signal-to-noise ratio, ultrathin sections were contrasted with 2 % uranyl acetate (Electron Microscopy Sciences) in 50 % ethanol (Molar) and 2 % lead citrate (Electron Microscopy Sciences) in distilled water. All the samples were systematically screened at 3000× magnification to localize the individual algal cells on the grid. Afterwards, images of algae were recorded at 10,000–50,000× magnification with a 16 MPx Matataki Flash scientific complementary metal–oxide–semiconductor camera (JEOL).

Using the built-in profile tool of the JEOL TEM Center software, relative distances between thylakoids were measured in silico. First, the center of the black line representing the grana stack membrane and lumen was selected, followed by the center of the subsequent grana stack. The distance between the two grana stacks with the stromal space was then expressed as repeat distance [23].

For perimeter measurement, microscopic images were opened in Image J software, the scale was adjusted, the boundaries of the algal cells were defined by polygonal selection and perimeter measurements were performed. 50 cells were randomly selected for each measurement.

2.3. Circular dichroism (CD) spectroscopy

CD spectra were recorded on a Jasco J-815 CD spectropolarimeter at room temperature with a bandwidth of 2 nm and data pitch of 1.0 nm. The scan speed was set to 100 nm/min and the integration time was 1 s. Simultaneously with the CD spectra, absorption spectra were recorded as well and the CD spectra were normalized to the red absorbance maxima, at around 680 nm. 750 nm reference wavelength was used to determine the amplitude of the $(+)690$, $(-)675$ and $(+)505$ psi-type CD (CD_{Ψ}) bands (psi, polymer or salt induced). The chlorophyll concentration of the samples was 30 μg/mL. Five independent biological replicates were measured.

2.4. Fast chlorophyll-a fluorescence (OJIP) transients

Fast chlorophyll-*a* (Chl-*a*) fluorescence measurements were carried out at room temperature with a Handy-PEA instrument (Hansatech Instruments Ltd., UK). The cells were dark acclimated for 15 min and then 3 mL of cell suspension (10 μg Chl mL^{-1}) was filtered onto a Whatman glass microfiber filter (GF/B). The sample was illuminated with continuous red light (3500 μmol photons m^{-2} s^{-1}) for 3 s. The first reliably measured point of the fluorescence transient is at 20 μs, which was taken as Fo.

2.5. Measurement of reactive oxygen species

Cell-permeant 2′,7′-dichlorodihydrofluorescein diacetate (DCFH-DA) was used to detect the generation of reactive oxygen intermediates by measuring the fluorescence of 2′,7′-dichlorofluorescein (DCF) in every 30 min by a HIDEX plate reader using the following settings: excitation wavelength/bandwidth: 490/20 nm, emission wavelength: 520/14 nm. 15 mL of algal cultures were centrifuged and washed with 20 mM K-P buffer pH 7 and then resuspended in 20 mM K-P buffer pH 7. The cells were incubated at 25 °C in dark by shaking at 180 rpm for 1 h. After centrifugation the cells were washed with TAP and resuspended in 7.5 mL of TAP. 120 μL of 0.5 mM DCFH-DA (5 μM final concentration)

was added to 6 mL suspension, then the suspension was aliquoted into 24-well microtiter plate containing salt-free TAP media or TAP media with NaCl. The remaining 1.5 mL of suspension was used for control samples lacking the fluorescent dye. The plates were incubated at 25 °C under 50 μmol photons m^{-2} s^{-1} light intensity by shaking at 180 rpm. In every 30 min fluorescence measurement was done in a HIDEX plate reader to determine the DCF levels.

2.6. Statistical analysis

The experimental data were processed using the GraphPad Prism software, and the values were expressed as mean ± SEM. All data were subjected to *t*-test analysis. *P*-value <0.05 was considered significant difference.

3. Results

3.1. Growth characteristics of microalgae under saline conditions

Chlamydomonas reinhardtii cc124, *Chlorella* sp. MACC-360 and *Coelastrella* sp. MACC-549 algal strains were cultivated in 24-well microtiter plates in TAP medium containing various concentrations of NaCl (Fig. 1). The algal strains were challenged with salt concentrations ranging between 0.1 and 1 M. Strikingly different tolerance values were observed for the various algae. *C. reinhardtii* was able to tolerate salt concentrations up to 0.2 M NaCl (henceforth, referred to as maximum salt tolerance value) (Fig. 1A). *Chlorella* sp. MACC-360 tolerated significantly higher concentration of salt with a maximum tolerated salt concentration of 0.6–0.65 M (Fig. 1B). The tolerance of *Coelastrella* sp. MACC-549 to salt was higher compared to that of the *Chlamydomonas* strain (with a maximum tolerated NaCl concentration of 0.35 M) (Fig. 1C). As a general observation, the elevated salt concentration resulted in increased cell aggregation for all tested algal strains. Cell counting supported the simple visual observation of algal growth in the 24-well microtiter plates (Fig. 2). *C. reinhardtii* cc124 cell counts were suddenly dropped by orders of magnitudes above 0.2 M salt
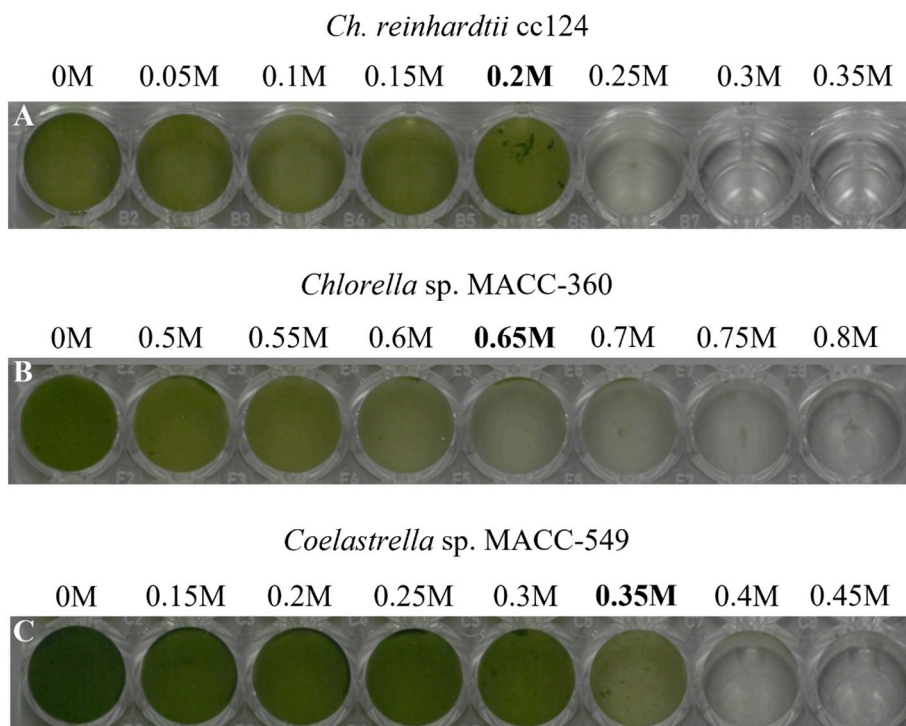

Fig. 1. Microplate cultivation of microalgae under various salt concentrations. A. *C. reinhardtii* cc124 cultivated in TAP containing 0 to 0.35 M NaCl; B. *Chlorella* sp. MACC-360 cultivated in TAP containing 0 to 0.8 M NaCl; C. *Coelastrella* sp. MACC-549 cultivated in TAP containing 0 to 0.45 M NaCl. All cultures were 7-day old.
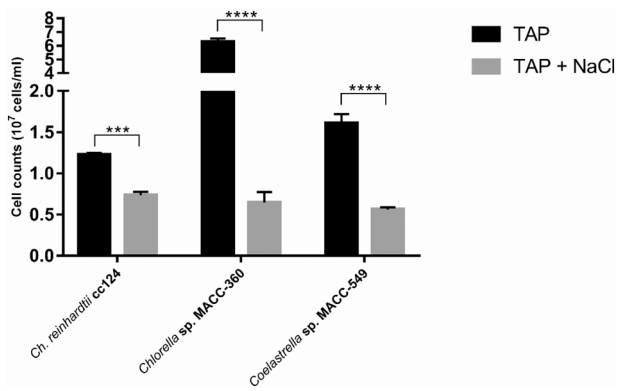
Fig. 2. Algae live cell counts after 7 days of growth at the maximum tolerated NaCl concentrations for each alga. *C. reinhardtii* cc124 cell counts were measured in TAP (black) and in TAP containing 0.2 M NaCl (grey). *Chlorella* sp. MACC-360 cell counts were measured in TAP (black) and in TAP containing 0.65 M NaCl (grey), and *Coelastrella* sp. MACC-549 cell counts were measured in TAP (black) and in TAP containing 0.35 M NaCl (grey).

concentration, while cell counts of *Chlorella* sp. MACC-360 showed a rather gradual decrease even above 0.65 M NaCl. Like *C. reinhardtii* cc124 the *Coelastrella* sp. MACC-549 cell counts decreased dramatically above its maximum salt tolerance value of 0.35 M (Supplementary Table 1 and Supplementary Fig. 1).

3.2. Morphological changes and EPS production of microalgae in response to salt stress

The morphology and cellular structure of the salt-treated algae were investigated using various microscopic techniques. A number of characteristic structural changes were observed for each algal strain. As expected, the *Chlamydomonas* cells briefly lost their flagella and showed clear aggregation in response to elevated salinity as observed through scanning electron microscopy (Fig. 3AB). The palmelloid structure became clearly dominant already at 0.2 M salt concentration as revealed by scanning electron microscopy (Fig. 3AB). Confocal laser scanning microscopy (CLSM) was used to investigate the cell wall content and to detect the potential salt-promoted changes in the production and accumulation of extracellular matrix components. Seven-day-old microalgal cells were stained with calcofluor white (CFW) and concanavalin A (Con A) dyes (Fig. 4). CFW dye binds to polysaccharides composed of β-D glucopyranose units, while Con A binds to the α-D
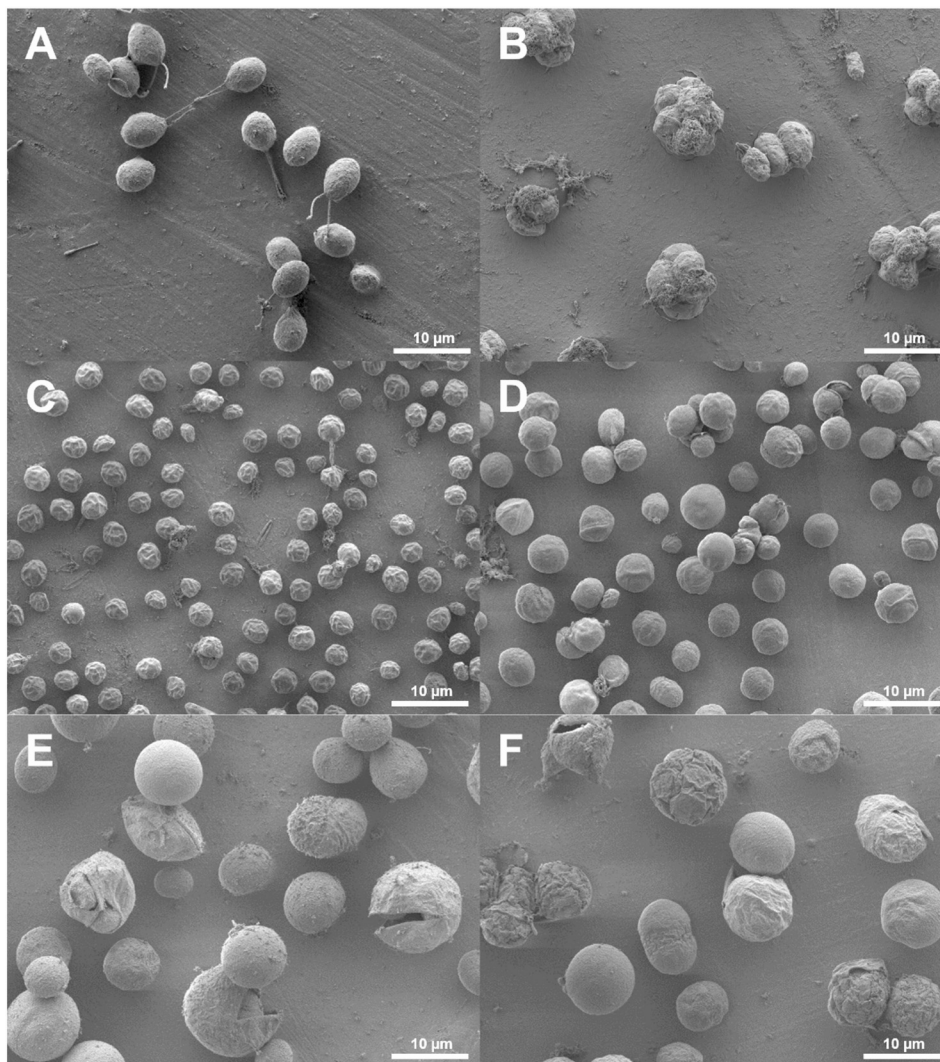

Fig. 3. Scanning electron microscopy observation of algal cells under various salt concentrations. A. *C. reinhardtii* cc124 in TAP medium; B. *C. reinhardtii* cc124 in TAP containing 0.2 M NaCl; C. *Chlorella* sp. MACC-360 in TAP; D. *Chlorella* sp. MACC-360 in TAP containing 0.65 M NaCl; E. *Coelastrella* sp. MACC-549 in TAP; F. *Coelastrella* sp. MACC-549 in TAP containing 0.35 M NaCl.

glucopyranose-based polysaccharides. Palmelloid formation of *C. reinhardtii* cc124 cells was clearly visible with ConA staining, which confirmed the morphology changes observed by SEM (Fig. 4A). The cell wall composition of *C. reinhardtii* cc124 did not show any changes in response to salt stress as indicated by green fluorescence of ConA (Fig. 4A), while the cells size of the individual algal cells within the palmelloid sheath showed a moderate decrease (Fig. 4D). The *Chlorella* sp. MACC-360 cells showed strikingly different responses to the elevated salt concentration (Fig. 3 CD). The cells showed only a slight aggregation even at 0.65 M salt concentration, only a few palmelloid-like structures could be identified, most of the cells retained their unicellular formation. However, the size of the individual *Chlorella* cells increased substantially compared to those in the salt free TAP medium (cell perimeter values increased by 150 % as calculated from the CLSM images) (Fig. 3CD, Fig. 4BD). Interestingly, *Chlorella* sp. MACC-360 microalgal cells secreted lots of polysaccharides when cultivated in salt-free TAP as shown by ConA staining, however this EPS production was fully terminated in the presence of 0.65 M NaCl (Fig. 4B). It is to note that the cell wall of *Chlorella* sp. MACC-360 could be stained only with CFW indicating the different carbohydrate content of the cell wall structures in *Chlamydomonas* and *Chlorella* species (Fig. 4AB). The *Coelastrella* sp. MACC-549 cells showed the least morphological changes in response to increased salt concentrations (Fig. 3EF). The large average cell size of the *Coelastrella* algae showed significant variations in the salt free medium as well; this feature remained unaltered in the high salt medium; the average cell size values showed slight decrease in response to salt stress (Fig. 4D). The unicellular nature of the cells was also quite stable, and the characteristic wrinkled cell wall of this algal strain was also maintained under elevated saline concentrations. The most specific response of the *Coelastrella* sp. MACC-549 cells to the increased salt concentration was the alteration of the cell wall composition (Fig. 4C). While only ConA dye was able to stain the *Coelastrella* cell wall when grown in TAP, the glucopyranose carbohydrate units of the cell wall underwent conformational changes in response to salt addition to TAP, which was clearly shown by the strong CFW fluorescent signal (and the ConA green fluorescence became much weaker) (Fig. 4C).

3.3. Differential effects of salt on microalgal lipid production

The effect of high salt concentration on the lipid production of various green microalgae was also investigated. No significant change was observed in the lipid production of *C. reinhardtii* cc124 under various salt concentrations (Fig. 5A). However, strong blue colour showed the increased lipid production of *Chlorella* sp. MACC-360 cells under high salt condition as revealed by BODIPY staining (Fig. 5B). To the contrary, in *Coelastrella* sp. MACC-549 cells the lipid content strongly decreased within the cells under high salt conditions compared to the cells grown in TAP (Fig. 5C).

3.4. High saline condition influences the ultrastructure of algal cells

Transmission electron microscopy was applied to further visualize the effects of salt treatments on the morphology of the algal cells and the ultrastructure of their thylakoid membranes (Fig. 6). The *C. reinhardtii* cc124 cells showed significant alteration in their shape at 0.2 M NaCl treatment, the individual cells became more rounded within the joint palmelloid sheath and enlarged pyrenoids surrounded by large starch granules were observed (Fig. 6AB). The strong size increase of the individual *Chlorella* cells was also confirmed by TEM, as well as clearly thicker cell wall and starch accumulation were also characteristic features of the *Chlorella* cells under elevated salt concentrations of 0.65 M (Fig. 6CD). The *Coelastrella* sp. MACC-549 cells did not exhibit major alteration in their shape and size, however, clearly thicker cell wall and starch accumulation were observed in this alga at 0.35 M NaCl treatment (Fig. 6EF). The repeat distance of the thylakoid membranes calculated from electron micrographs showed a reduction in the case of salt-treated

algal cells with reference to the controls for each strain (Fig. 7). This shrinkage of thylakoid structures was the most obvious for the *Chlamydomonas* and *Coelastrella* cells, this observation agrees well with the detected perturbations of the photosynthetic machinery in these two algae (see later in Figs. 8 and 9).

3.5. Effect of high salinity on the structure and function of the photosynthetic apparatus

Two non-invasive biophysical techniques, CD spectroscopy and fast Chl-*a* fluorescence induction kinetics were applied to inspect the effects of salt treatments on the structure and function of the photosynthetic machinery of live algal cells. Salt concentrations slightly below the observed maximum tolerance values (described above) were applied for the three algal strains (0.15 M NaCl for *C. reinhardtii* cc124 and for *Coelastrella* sp. MACC-549 and 0.5 M NaCl for *Chlorella* sp. MACC-360).

The CD spectra revealed no significant alterations in the excitonic bands (at around 650 nm and in the Soret regions), originating from short-range pigment-pigment interactions in the pigment-protein complexes; these signals predominantly arise from LHCII (light harvesting complex II) (Fig. 8).

It was clear that – with the exception of *Chlorella* sp. MACC-360 – already a moderate NaCl treatment (0.15 M) substantially perturbed the long-range order of the protein complexes, i.e. the macro-array of LHCII and PSII (Photosystem II):LHCII supercomplexes, as reflected by changes in the main CD_Ψ bands peaking at around (+)690, (−)675 and (+)505 nm. This might be the consequence of changes in the ionic composition and strength, which perturb the predominantly Mg^{2+}-mediated stacking interactions [24]. Interestingly, in all cases the amplitude of the (+)505 nm CD_Ψ band appeared to be sensitive to the applied salt treatments, which might originate from alterations in the carotenoid composition and/or in the organization of the PSII:LHCII supercomplexes [25]. The results obtained at various salt concentrations for the various algal strains suggested that (i) the compensation mechanism operating in *Chlorella* sp. MACC-360 was much more robust compared to the *Chlamydomonas* and *Coelastrella* algae; and (ii) the elevated ionic strength and/or the altered ionic composition affected the carotenoid composition of the PSII:LHCII supercomplexes.

The measurement of the OJIP transients (see details in the Discussion section) are sensitive indicators of the activity and dynamics of PSII and the operation of the electron transport system and are commonly used to characterize stress-induced effects on PSII or the entire electron transport system. The OJIP transients data of *Chlamydomonas reinhardtii* cc124 and *Coelastrella* sp. MACC-549 showed that their PSIIs suffered some damage or underwent minor reorganization, as indicated by the statistically significant decrease in the Fv/Fm parameter (Fig. 9AC), albeit the photosynthetic activity of these algae was largely retained in the presence of 0.15 M NaCl, as reflected by the OJIP transients. No such difference could be discerned in *Chlorella* sp. MACC-360 despite the more than three-fold NaCl concentration (0.5 M) applied in the growth medium (Fig. 9B). In this *Chlorella* strain only a relatively small salt-induced enhancement of the O-J step was observed, which could be caused by a moderately enhanced basal ion flux in the presence of 0.5 M NaCl [26,27].

Although the decreased Fv/Fm values in the two salt-sensitive species (*Chlamydomonas* and *Coelastrella*) were similar, the underlying mechanisms might be different. In *C. reinhardtii* cc124 the so-called photochemical (O-J) phase was hardly affected by NaCl, while in *Coelastrella* sp. MACC-549 cells the rate of the O-J step was significantly decelerated (Fig. 9AC). This difference might originate from differences in the Q_A-to-Q_B electron transfer rate or, more likely, from the salt stress induced structural dynamics alterations of PSII. It is worth noting that the two strains displayed strikingly different OJIP patterns in the control salt free samples as well. The origin of this difference is most likely family-specific, the Chl-a fluorescence induction parameters also exhibit large variations among aquatic oxygenic photosynthetic organisms [28].
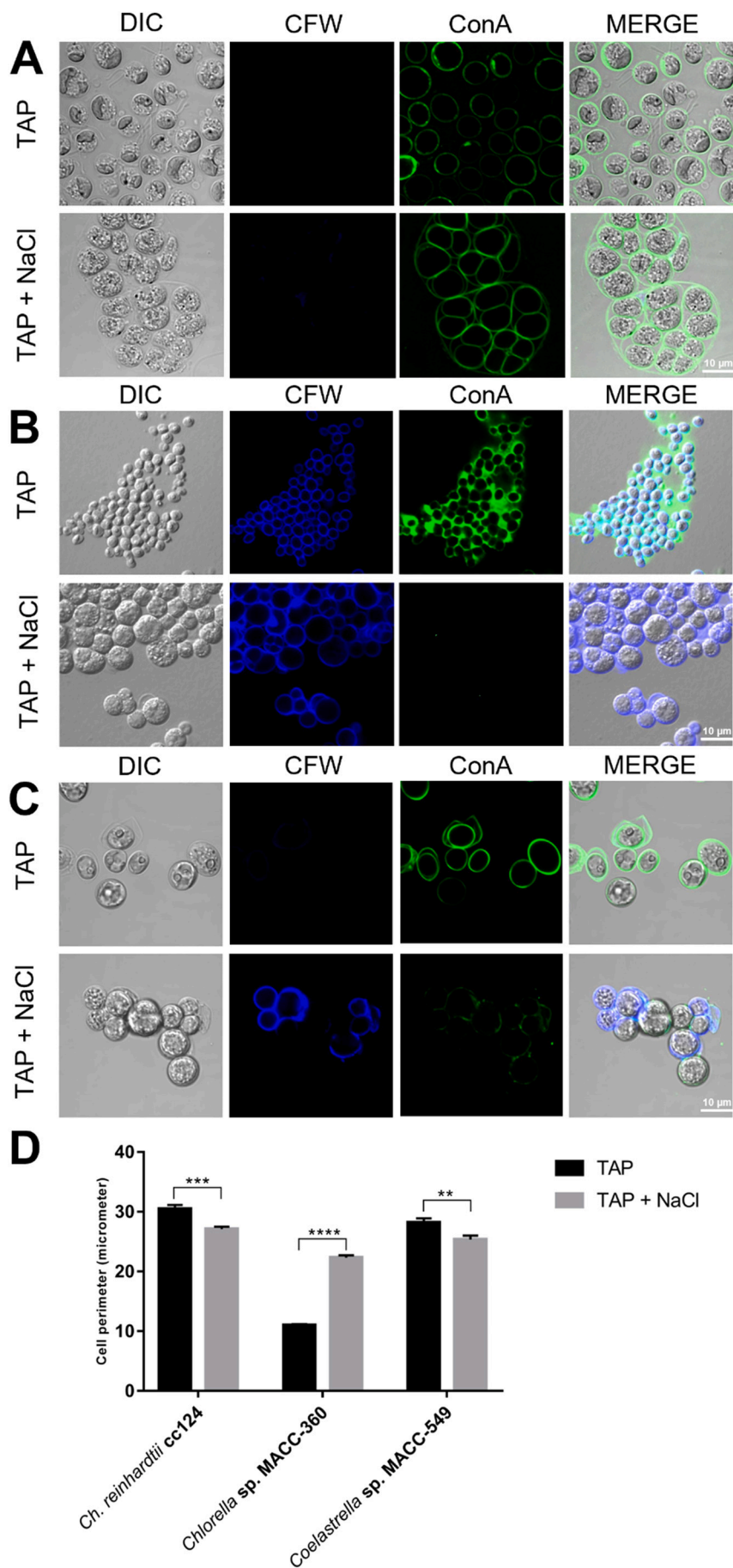
Fig. 4. CLSM pictures of live microalgal cells under various salt concentrations. The algal cells were stained with calcofluor white (CFW) and concanavalin A (Con A). DIC (differential interference contrast) and fluorescent pictures were merged as well. A. *C. reinhardtii* cc124 in TAP and TAP containing 0.2 M NaCl; B. *Chlorella* sp. MACC-360 in TAP and TAP containing 0.65 M NaCl; C. *Coelastrella* sp. MACC-549 in TAP and TAP containing 0.35 M NaCl. D. Individual cell perimeter values were measured on cells within the palmelloid sheath.
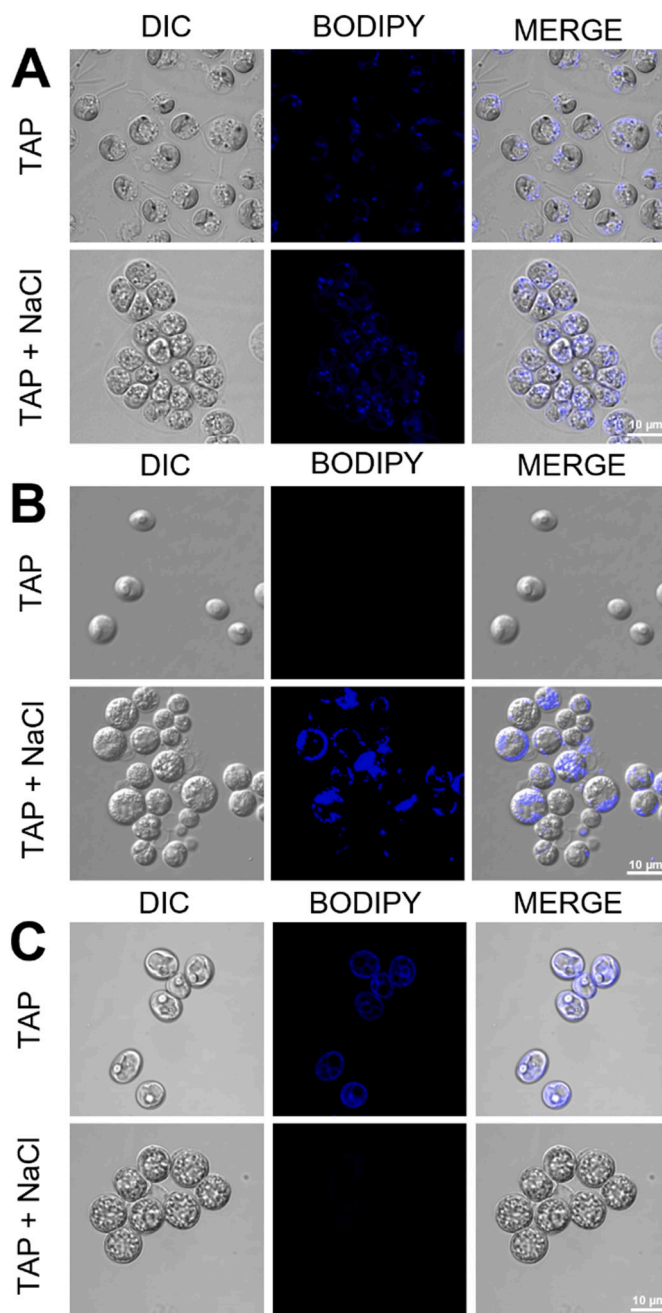
Fig. 5. Visualization of neutral lipid content of the algal cells. DIC (differential interference contrast) and fluorescent pictures were merged as well. A. *C. reinhardtii* cc124 in TAP and TAP containing 0.2 M NaCl; B. *Chlorella* sp. MACC-360 in TAP and TAP containing 0.65 M NaCl; C. *Coelastrella* sp. MACC-549 in TAP and TAP containing 0.35 M NaCl.

3.6. Production of reactive oxygen species

Reactive oxygen species (ROS) are typically produced in algae in response to various abiotic stresses including increased salinity. ROS are cell signaling molecules synthesized mostly in the mitochondria within the cells and act as secondary messengers in numerous cellular processes. Under stress conditions the concentrations of various ROS increase several folds in the cells leading to an accelerated cell aging phenotype. 2′,7′-dichlorodihydrofluorescein diacetate (DCFH-DA) is a non-fluorescent, cell-permeable dye which is hydrolyzed intracellularly into its polar, non-fluorescent form of DCFH (2′,7′-dichlorodihydrofluorescein) through the action of intracellular esterases. Oxidation of

DCFH by the action of intracellular ROS (including mostly peroxides) turns the molecule into its highly fluorescent form of 2′,7′-dichlorofluorescein (DCF) that can be detected by various fluorescent methods [29–31]. The exposure of algal cells to salt stress induced an increase in the intracellular ROS levels in *Chlamydomonas* and *Chlorella* (Fig. 10.). After 90 min, differences were observed for these two algal strains between the fluorescence of cells resuspended in medium containing elevated salt concentration and those in salt free TAP medium. These differences were significant for *C. reinhardtii* cc124 and for *Chlorella* sp. MACC-360; interestingly, the highest ROS levels were measured for *Chlorella* sp. MACC-360, which was shown to exert the highest tolerance against salt stress in the previous experiments. To the contrary, no significant DCF fluorescence changes were observed in the case of *Coelastrella* sp. MACC-549 between salt stressed and normal conditions implying that most likely diverse molecular mechanisms are involved in the mitigation of salt stress in the various Chlorophyta algae.

4. Discussion

For the past few years, we have learnt more and more information on how microalgae might respond to various adverse conditions. The major goal of this study was the investigation of the specific physiological responses of three selected freshwater eukaryotic green algal strains to stress caused by high salinity conditions. Chlorophyta algae are important participants in the global biogeochemical cycle, and they also play important roles in industrial settings and wastewater treatment. A more comprehensive understanding of their responses to abiotic stresses such as salinity, might provide insights into how to optimize their utilization. Additionally, chlorophytes and embryophytes are closely related, sharing a common ancestor. They display similar responses to phytohormones and abiotic stresses, making chlorophytes excellent model organisms for studying higher plants as well.

Coping with high salinity stress requires drastic changes in algae morphology and osmolyte concentrations in the short-term and accumulation of advantageous mutations in the long run. Here we were focusing on the introduction of diverse short-term measures taken by selected eukaryotic freshwater green algae species to maintain cell homeostasis and ability to propagate. It is not surprising that a sudden change in the osmotic conditions quickly limits the growth and propagation of unicellular freshwater algae. *C. reinhardtii* cells under high salt stress have much lower growth rate compared to untreated cells. The cells were smaller in the dividing stage across all the salt concentrations [32]. Increasing salt concentrations negatively affected the growth of other freshwater algae species such as *Chlorella vulgaris*, *Chlorella salina*, *Chlorella emersonii* [33], and *Scenedesmus opoliensis* [34]. However, the inhibiting concentration of saline was highly variable among various green algae species. Among the three investigated green algae species, *Chlorella* sp. showed the highest tolerance against increasing salinity, the growth of the *Chlorella* sp. was unaffected up to 0.6 M NaCl concentration (Fig. 1 A, Fig. 2 and Supplementary Table 1). On the contrary, strong growth limitation was detected for both *C. reinhardtii* cc124 and *Coelastrella* sp. MACC-549 at saline concentrations above 0.2 and 0.35 M, respectively (Fig. 1 BC, Fig. 2 and Supplementary Table 1).

C. reinhardtii cells exposed to unfavorable high saline conditions entered a temporarily multicellular stage termed as palmelloid. The palmelloid morphology was highly visible, these multicellular structures were visualized using scanning electron (SEM) and fluorescent (CLSM) microscopy techniques (Figs. 3-5). Multiple changes occurred in the structure of the *Chlamydomonas* cells including the rapid loss of flagella, the cells clustered together with a minimum of two cells per cluster, the clustered cells shared a common sheath and the size of the individual cells showed a moderate decrease. Ultrastructural changes were also observed, enlarged pyrenoids surrounded by large starch granules were observed, and significant decrease in the repeat distance of thylakoid membranes was measured (Figs. 6 and 7). The palmelloids quickly accumulated in the first 24 h after exposure to high salinity.
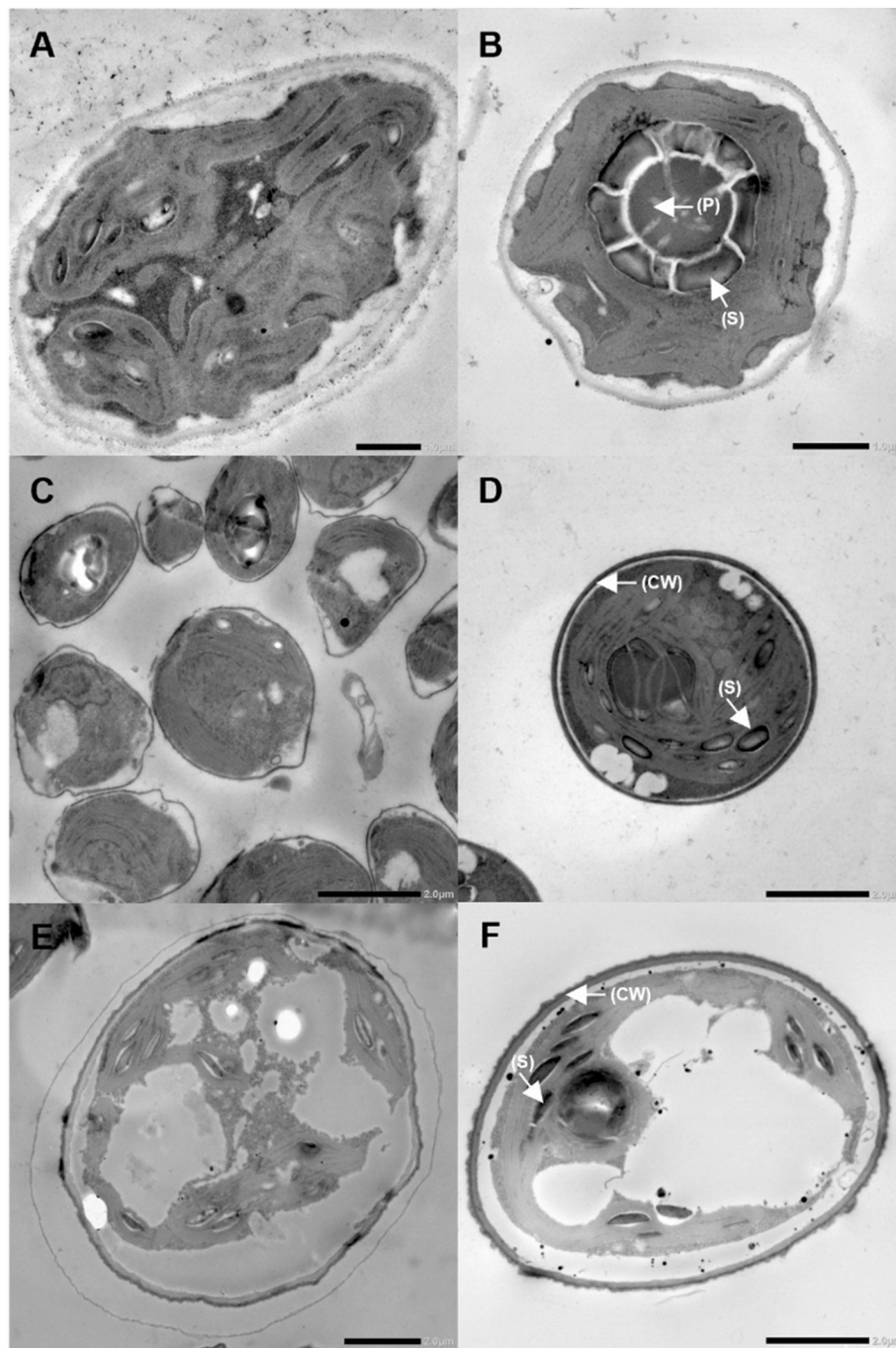
Fig. 6. Transmission electron microscopy observation of algal cells under various salt concentrations. A. *C. reinhardtii* cc124 in TAP medium; B. *C. reinhardtii* cc124 in TAP containing 0.2 M NaCl; C. *Chlorella* sp. MACC-360 in TAP; D. *Chlorella* sp. MACC-360 in TAP containing 0.65 M NaCl; E. *Coelastrella* sp. MACC-549 in TAP; F. *Coelastrella* sp. MACC-549 in TAP containing 0.35 M NaCl. Scale bar: 2 μm.

The palmelloid stage results from daughter cells remaining attached to one another after cell division, as opposed to free swimming cells aggregating into palmelloids. EPS secretion frequently accompanies palmelloidy, with daughter cells embedded in the EPS matrix. This matrix dissolves swiftly under favorable conditions due to the activity of specific metalloproteinases [13]. Palmelloidy is frequently observed in *Chlamydomonas* cells exposed to different abiotic stresses including: phosphate limitation [35], exposure to organic acids [11], predator grazing [36] and herbicide exposure [37]. The larger size of the palmelloids enables *Chlamydomonas* to surpass the predator's ingestion size, allowing the alga to survive herbivore predation and increase its chances for survival. However, it is important to mention that studies have also confirmed variable viability of cells within palmelloids. NaCl induced palmelloids of *C. reinhardtii* CC-125 showed decreased viability after 48 h [38] while palmelloids of *C. eugametos* and *C. applanata* survived for up to 5 days [39].

A proteomic analysis identified a number of proteins likely to be linked to palmelloid formation (expansin, wall stress-responsive component (WSC) domain protein, pheophorin-C5, vegetative storage protein (VSP4), and cathepsin-Z-like proteins) [38]. The selected representatives of *Chlorella* and *Coelastrella* genera did not form palmelloids, these green algae showed different mechanisms to tackle with salt stress. Extreme increase was observed in the cell size and volume of the investigated *Chlorella* sp. MACC-360 strain. This was especially unusual
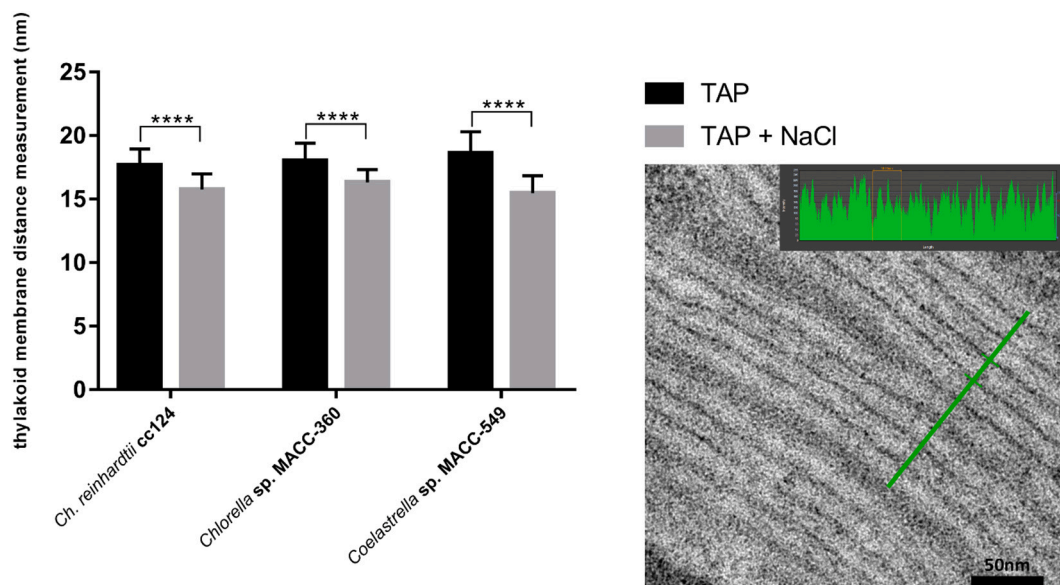
Fig. 7. Repeat distance values of thylakoid membranes in algal cells cultivated under various salt concentrations. *C. reinhardtii* cc124 strain was cultivated in TAP (black) and in TAP containing 0.2 M NaCl (grey). *Chlorella* sp. MACC-360 was grown in TAP (black) and in TAP containing 0.65 M NaCl (grey), and *Coelastrella* sp. MACC-549 was grown in TAP (black) and in TAP containing 0.35 M NaCl (grey). Picture on the right side illustrates how repeat distance values between thylakoids were measured (see details in the Material and Methods section). All values are shown in nm.
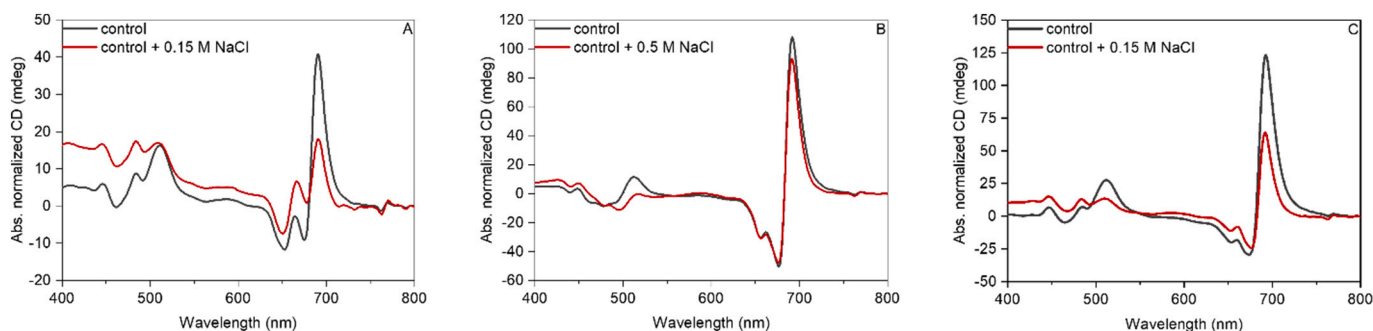

Fig. 8. Representative circular dichroism spectra of untreated control (black) and salt-treated (red) *C. reinhardtii* cc124 (A), *Chlorella* sp. MACC-360 (B) and *Coelastrella* sp. MACC-549 (C) algal cells, respectively. The spectra are normalized to the corresponding red absorbance maxima [$OD_{680} = 1.0$] of the samples. Five independent biological replicates were measured and typical data sets are shown. (For interpretation of the references to colour in this figure legend, the reader is referred to the web version of this article.)
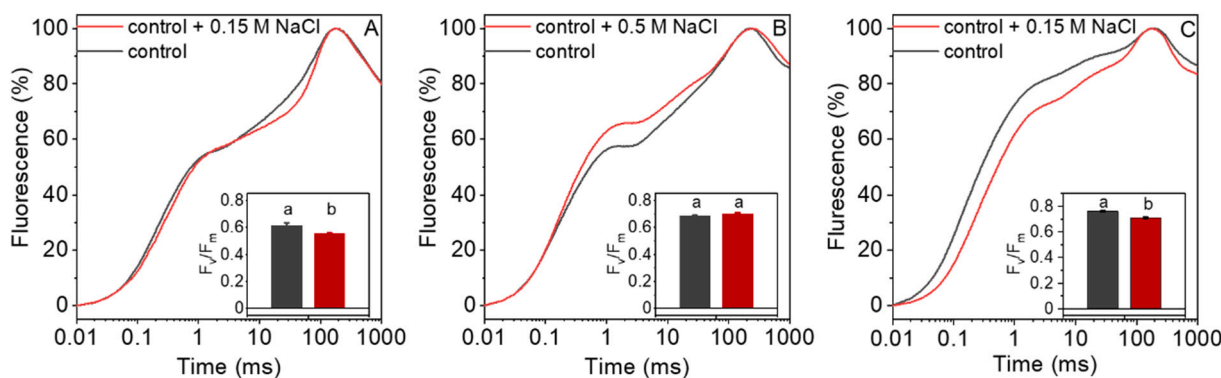

Fig. 9. Effect of NaCl on the fast Chl-a fluorescence (OJIP) transients of untreated control (black) and salt-treated (red) *C. reinhardtii* cc124 (A), *Chlorella* sp. MACC-360 (B) and *Coelastrella* sp. MACC-549 (C) algal cells. The kinetic traces represent the averages from five independent experiments on different batches. The traces are normalized to Fo (O, minimum) and Fm (P, maximum) fluorescence levels. The insets show the F_v/F_m values; mean values $\pm$ SE from five independent experiments on different batches. Different (a and b) letters indicate statistically significant differences (ANOVA with Bonferroni post-hoc test, $P < 0.05$). (For interpretation of the references to colour in this figure legend, the reader is referred to the web version of this article.)
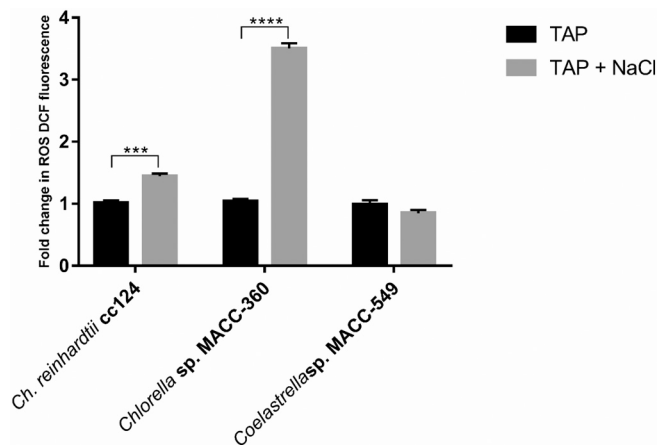
Fig. 10. Production of Reactive Oxygen Species (ROS) in the algal cells in response to salt stress. ROS accumulation in the various algal strains were detected by fluorescence intensity measurement using 2′,7′-dichlorodihydro-fluorescein diacetate (DCFH-DA). DCF fluorescence intnstities were recorded for *C.. reinhardtii* cc124 in TAP medium and in TAP containing 0.2 M NaCl; for *Chlorella* sp. MACC-360 in TAP medium and in TAP containing 0.65 M NaCl; and for *Coelastrella* sp. MACC-549 in TAP medium and in TAP containing 0.35 M NaCl, respectively.

and unexpected since *Chlorella* species are considered to maintain a rigid and thick cell wall, thus limiting its ability to change cell volume (thickened cell wall was observed in our experiments as well using TEM for the ultrastructural investigations).

Similar increase in algal cell size has been observed in previous studies in response to salt stress. The diameter of *C. sorokiana* HS1 [40] doubled and there was a significant increase in the cell size of *Chlorella vulgaris* UTEX2714 [41] under high salinity. Increased *Chlorella* cell size in salt-treated cultures may also be explained by lack of cell division, however, this hypothesis has to be confirmed by ongoing studies. Another hypothesis suggests that osmosensing and osmoregulation are likely to induce metabolic changes, which then influence cell volume and biochemical composition [41].

Similar rapid change of cell volume was observed for *Dunaliella salina* green algae, which lacks a rigid cell wall allowing the algal cells to expand in response to high salinity stress. A study on cell size changes in *D. salina* caused by high salt stress showed continuously fluctuating cell volumes for several days, which finally stabilized at a slightly larger size compared to the stress-free condition [42].

The *Coelastrella* sp. MACC-549 strain did not exhibit any major morphological changes under high salt conditions; however, clearly altered and thickened cell wall structure was identified in *Coelastrella* cells compared to that under salt-free conditions, as revealed by fluorescent and electron microscopy techniques (differential staining with ConA and CFW shed light on the conformational changes of the glucopyranose carbohydrate units of the cell wall in response to salt stress). It is to note that EPS production was only slightly affected in the tested algal strains. Fluorescent microscopy experiments also revealed that the investigated *Chlamydomonas* and *Coelastrella* algae did not produce any visible EPS under any tested conditions, while the excessive amount of EPS - visible through concanavalin-A staining - produced by *Chlorella* sp. MACC-360 in TAP medium could not be detected any more in the cultures grown in TAP supplemented with NaCl. The *Chlorella* sp. MACC-360 alga exhibited a lipid-producing phenotype under high salt conditions; thus, salt stress provoked neutral lipid production of this strain. *Chlorella* sp. MACC-360 exhibited lipid droplets under high salt conditions indicating that salt stress induced lipid production in this particular alga. Previous studies have shown that salt stress could increase the lipid content of *Chlorella*, likely due to modifications to the cell membrane and regulation of lipid metabolism caused by the osmotic stress.

Lipid accumulation takes place in specialized organelles called lipid droplets (LD) [43]. Lipid droplets contribute to salt tolerance in green algae. The disappearance of accumulated lipid droplets in *Chlamydomonas* and *Parachlorella* is accompanied by the re-synthesis of photosynthetic membranes and re-gain of vegetative growth [14,44]. The growth of *Parachlorella* is also correlated with LD content, the LDs contribute to the rapid reconstruction of organelles when stress conditions are ceased. The increase of lipid content can lead to glycerol production, which plays an important protective role as an organic osmolyte and fatty acid source. Thus, lipid-producing phenotype might have immense exploitative significance. Another anticipated and frequent stress response of increased ROS production was observed in *Chlamydomonas* and *Chlorella* (this increase was especially high in *Chlorella* sp. MACC-360), while in *Coelastrella* MACC-549 no such response was recorded.

Regarding the effects of salt stress on the photosynthetic machineries, some common features and differences can be recognized. Decrease in the thylakoid membrane repeat distances was observed in all algal strains, with some statistically significant differences (Fig. 7). These can most probably be attributed to the elevated ionic strengths in the chloroplasts. Indeed, decreased thylakoid repeat distances have been induced by changing the osmotic medium of 0.4 M sorbitol to 0.3 M NaCl in a suspension of isolated tobacco thylakoid membranes [45]. Shrinkage in the thylakoid membrane system may perturb the chiral macro-organization of the pigment-protein complexes, explaining the diminshed amplitudes of CD$_\Psi$ bands (Fig. 8). These bands originate from large three-dimensional macroaggregates containing high density of interacting chromophores [46]; and thus, they are sensitive to changes in the multilamellar organization of the membranes [47]. It is interesting to note, that, in harmony with the order of the salt tolerances, *C. reinhardtii* cc124 suffered the largest CD$_\Psi$ losses, followed by *Coelastrella* sp. MACC-549; while in *Chlorella* sp. MACC-360 cells only the (+) 505 nm band was suppressed, with no or little effects in the red (Fig. 8). It is also noteworthy that the reverse order can be discerned in the (−) 675 nm CD amplitudes of the untreated cells. This CD$_\Psi$ band has been shown to reflect the strength of stacking [24]. Hence, it appears that in *Chlorella* sp. MACC-360 the robust macro-organization of the pigment-protein complexes in the thylakoid membranes, stabilized by stacking, may play a role in the salt tolerance of these cells.

Changes in the macro-organization of the thylakoid membrane system and the pigment-protein complexes may also affect the functional activity of PSII and the electron transport processes. Indeed, it has been shown that swelling of the lumenal space facilitates the diffusion of plastocyanin, which thus enhances the rate of electron transport between the two photosystems [48]. Conversely, shrinkage of the thylakoid membrane system – if, in part or fully caused by a decrease in the lumenal volume – would inhibit the electron transport from PSII to PSI, which is expected to modify the JIP transients [46]. However, there is no clear correlation between the shrinkage of thylakoid membranes, which occurs in all three strains (Fig. 7), and the salt-induced variations in the OJIP kinetic traces (Fig. 9) – suggesting the involvement of more complex mechanisms. Chlorophyll-a fluorescence transients depend both on the photochemical activity of PSII, with its open or closed states modulated by the linear electron transport [46], and the formation of the light-adapted charge-separated (closed) state [47]. When comparing the observed species-to-species variations of the OJIP transients and their respective salt-induced changes, it is evident that the kinetic traces differ more between the strains than between the control and the salt stressed sample of the same algal species. The elucidation of this question is outside the scope of the present work. Concerning the F$_v$/F$_m$ parameter (Fig. 9, inset), it is interesting to point out that it decreases significantly in the two sensitive strains, i.e. in the *C. reinhardtii* cc124 and the *Coelastrella* sp. MACC-549 cells This can be attributed to salt-stress induced damage in the structure and/or dynamics of PSII. In contrast, no such damage can be discerned in *Chlorella* sp. MACC-360, which might reflect the salt tolerances of its PSII, but it may also

originate from a more efficient repair mechanism of this photosystem [49]. Since, PSII is the source of all the reducing equivalents in the cell, maintaining its functional state might be of fundamental importance in salt tolerance of algae.

Several valuable products are generated by microalgae to enhance their survival under increased saline conditions. Salt stress promoted β-carotene production in *D. salina,* which is used as a colorant, food and feed additive [50]. Enhancing the production of glycerol or various exopolysaccharides (EPS) are also real possibilities [51]. Nevertheless, successful algae exploitation and engineered biomolecule production can only occur with a thorough understanding of the molecular mechanisms laying behind the flexibility and stress tolerance of various green algae species. Understanding the reasons and the molecular acclimation mechanisms of the different responses and highly diverse tolerance levels of Chlorophyta green algal strains will help in developing strategies to directly increase salt resistance in freshwater algae. Further investigation of their responses to environmental stressors will also deepen our understanding on plant evolution and provide valuable insights for agricultural and industrial applications.

5. Conclusion

This study investigated the ability of selected Chlorophyta green algae to grow and propagate under highly saline conditions. Differential species-specific salt-induced physiological, structural, and ultrastructural responses were identified in the investigated eukaryotic green algal strains. Specifically, *Chlorella* sp. MACC-360 demonstrated a remarkable increase in cell size, a significant reduction in EPS production, and substantial lipid body accumulation, while *Coelastrella* sp. MACC-549 exhibited thickened cell walls, and *C. reinhardtii* cc124 displayed the characteristic palmelloid formation. These results highlight the extensive diversity in microalgal responses and contribute to our understanding of the mechanisms underlying their acclimatization in saline conditions.

Chlorella sp. MACC-360 excelled with its outstanding salt-tolerance features showing robust growth properties up to 600 mM NaCl concentration. This halotolerant *Chlorella* strain can be useful for mass cultivation in nutrient media including wastewater of high and changing salinity. The robust biomass production phenotype together with its high salt condition-specific lipid production capability as well as the generally low sensitivity to abiotic stressors may make this green algal strain a key element in future biological desalination approaches.

CRediT authorship contribution statement

A.F. performed the experiments and led the microscopy analyses, B.P. performed the experiments, O.Zs. performed the CD spectroscopy and Chl-a fluorescence measurements, R.P. provided the TEM images, P.S. participated in the physiological analyses, G.G. provided useful hints and participated in the critical discussions, T.B. took part in the experimental design and literature review, V.Ö. provided recommendations for algal cultivation and discussed the results, G.M. designed the study and wrote the manuscript. All authors have read and agreed to the published version of the manuscript.

The authors also acknowledge the provided microscopy support of the Cellular Imaging Laboratory (Biological Research Centre, Eötvös Loránd Research Network).

Funding

Declaration of competing interest

The authors declare no conflict of interest.

Data availability

Data will be made available on request.

Appendix A. Supplementary data

Supplementary data to this article can be found online at https://doi.org/10.1016/j.algal.2023.103155.

References

[1] J.R.W. NORFOLK, Primary production of the biosphere, Biochem. Soc. Trans. 4 (1976) 954, https://doi.org/10.1042/bst0040954.
[2] M.I. Khan, J.H. Shin, J.D. Kim, The promising future of microalgae: current status, challenges, and optimization of a sustainable and renewable industry for biofuels, feed, and other products, Microb. Cell Factories 17 (2018) 1–21, https://doi.org/10.1186/s12934-018-0879-x.
[3] K. Kumar, S.K. Mishra, A. Shrivastav, M.S. Park, J.W. Yang, Recent trends in the mass cultivation of algae in raceway ponds, Renew. Sust. Energ. Rev. 51 (2015) 875–885, https://doi.org/10.1016/j.rser.2015.06.033.
[4] S. Fon Sing, A. Isdepsky, M.A. Borowitzka, D.M. Lewis, Pilot-scale continuous recycling of growth medium for the mass culture of a halotolerant *Tetraselmis* sp. in raceway ponds under increasing salinity: a novel protocol for commercial microalgal biomass production, Bioresour. Technol. 161 (2014) 47–54, https://doi.org/10.1016/j.biortech.2014.03.010.
[5] M. Huesemann, S. Edmundson, S. Gao, S. Negi, T. Dale, A. Gutknecht, H.E. Daligault, C.K. Carr, J. Freeman, T. Kern, S.R. Starkenburg, C.D. Gleasner, W. Louie, R. Kruk, S. McGuire, DISCOVR strain pipeline screening – part I: maximum specific growth rate as a function of temperature and salinity for 38 candidate microalgae for biofuels production, Algal Res. 102996 (2023), https://doi.org/10.1016/J.ALGAL.2023.102996.
[6] H.J.G. Meijer, J.A.J. van Himbergen, A. Musgrave, T. Munnik, Acclimation to salt modifies the activation of several osmotic stress-activated lipid signalling pathways in *Chlamydomonas*, Phytochemistry. 135 (2017) 64–72, https://doi.org/10.1016/j.phytochem.2016.12.014.
[7] I.J. Melero-Jiménez, E. Bañares-España, M.J. García-Sánchez, A. Flores-Moya, Changes in the growth rate of *Chlamydomonas reinhardtii* under long-term selection by temperature and salinity: acclimation vs. evolution, Sci. Total Environ. 822 (2022), https://doi.org/10.1016/j.scitotenv.2022.153467.
[8] P. Shetty, M.M. Gitau, G. Maróti, Salinity stress responses and adaptation mechanisms in eukaryotic green microalgae, Cells. 8 (2019) 1–16, https://doi.org/10.3390/cells8121657.
[9] A. Bafana, Characterization and optimization of production of exopolysaccharide from *Chlamydomonas reinhardtii*, Carbohydr. Polym. 95 (2013) 746–752, https://doi.org/10.1016/J.CARBPOL.2013.02.016.
[10] K. Iwasa, S. Murakami, Palmelloid formation of *Chlamydomonas* I. Palmelloid induction by organic acids, Physiol. Plant. 21 (1968) 1224–1233, https://doi.org/10.1111/j.1399-3054.1968.tb07353.x.
[11] K. Iwasa, S. Murakami, Palmelloid formation of chlamydomonas II. Mechanism of palmelloid formation by organic acids, Physiol. Plant. 22 (1969) 43–50, https://doi.org/10.1111/j.1399-3054.1969.tb07839.x.
[12] G.O. James, C.H. Hocart, W. Hillier, H. Chen, F. Kordbacheh, G.D. Price, M.A. Djordjevic, Fatty acid profiling of *Chlamydomonas reinhardtii* under nitrogen deprivation, Bioresour. Technol. 102 (2011) 3343–3351, https://doi.org/10.1016/j.biortech.2010.11.051.
[13] D.K. Khona, S.M. Shirolikar, K.K. Gawde, E. Hom, M.A. Deodhar, J.S. D'Souza, Characterization of salt stress-induced palmelloids in the green alga, *Chlamydomonas reinhardtii*, Algal Res. 16 (2016) 434–448, https://doi.org/10.1016/J.ALGAL.2016.03.035.
[14] Z. You, Q. Zhang, Z. Peng, X. Miao, Lipid droplets mediate salt stress tolerance in *Parachlorella kessleri*, Plant Physiol. 181 (2019) 510–526, https://doi.org/10.1104/pp.19.00666.
[15] K. Iwamoto, Y. Shiraiwa, Salt-regulated mannitol metabolism in algae, Mar. Biotechnol. 7 (2005) 407–415, https://doi.org/10.1007/s10126-005-0029-4.
[16] S.N.H. Oslan, N.F. Shoparwe, A.H. Yusoff, A.A. Rahim, C.S. Chang, J.S. Tan, S.N. Oslan, K. Arumugam, A. Bin Ariff, A.Z. Sulaiman, M.S. Mohamed, A review on *Haematococcus pluvialis* bioprocess optimization of green and red stage culture conditions for the production of natural astaxanthin, Biomolecules. 11 (2021) 1–15, https://doi.org/10.3390/biom11020256.
[17] T. Wang, H. Ge, T. Liu, X. Tian, Z. Wang, M. Guo, J. Chu, Y. Zhuang, Salt stress induced lipid accumulation in heterotrophic culture cells of *Chlorella protothecoides*: mechanisms based on the multi-level analysis of oxidative response, key enzyme activity and biochemical alteration, J. Biotechnol. 228 (2016) 18–27, https://doi.org/10.1016/j.jbiotec.2016.04.025.
[18] D.S. Gorman, R.P. Levine, Cytochrome f and plastocyanin: their sequence in the photosynthetic electron transport chain of *Chlamydomonas reinhardi*, Proc. Natl. Acad. Sci. U. S. A. 54 (1965) 1665–1669, https://doi.org/10.1073/pnas.54.6.1665.

[19] D.M. Kuhn, J. Chandra, P.K. Mukherjee, M.A. Ghannoum, Comparison of biofilms formed by *Candida albicans* and *Candida parapsilosis* on bioprosthetic surfaces, Infect. Immun. 70 (2002) 878–888, https://doi.org/10.1128/IAI.70.2.878-888.2002.

[20] M.Y. Chen, D.J. Lee, J.H. Tay, Distribution of extracellular polymeric substances in aerobic granules, Appl. Microbiol. Biotechnol. 73 (2007) 1463–1469, https://doi.org/10.1007/s00253-006-0617-x.

[21] G. Mar, *Chlamydomonas* Green Microalgae on *Medicago truncatula*, 2021, pp. 1–18.

[22] V. Rani, G. Maróti, Assessment of nitrate removal capacity of two selected eukaryotic green microalgae, Cells. 10 (2021), https://doi.org/10.3390/cells10092490.

[23] M. Li, R. Mukhopadhyay, V. Svoboda, H.M.O. Oung, D.L. Mullendore, H. Kirchhoff, Measuring the dynamic response of the thylakoid architecture in plant leaves by electron microscopy, Plant Direct. 4 (2020) 1–14, https://doi.org/10.1002/pld3.280.

[24] G. Garab, J. Kieleczawa, J.C. Sutherland, C. Bustamante, G. Hind, Organization of pigment-protein complexes into macrodomains in the thylakoid membranes of wild-type and chlorophyll fo-less mutant of barley as revealed by circular dichrosim, Photochem. Photobiol. 54 (1991) 273–281, https://doi.org/10.1111/j.1751-1097.1991.tb02016.x.

[25] T.N. Tóth, N. Rai, K. Solymosi, O. Zsiros, W.P. Schröder, G. Garab, H. Van Amerongen, P. Horton, L. Kovács, Fingerprinting the macro-organisation of pigment-protein complexes in plant thylakoid membranes in vivo by circular-dichroism spectroscopy, Biochim. Biophys. Acta Bioenerg. 2016 (1857) 1479–1489, https://doi.org/10.1016/j.bbabio.2016.04.287.

[26] T.K. Antal, V. Osipov, D.N. Matorin, A.B. Rubin, Membrane potential is involved in regulation of photosynthetic reactions in the marine diatom *Thalassiosira weissflogii*, J. Photochem. Photobiol. B Biol. 102 (2011) 169–173, https://doi.org/10.1016/j.jphotobiol.2010.11.005.

[27] B. Ughy, V. Karlický, O. Dlouhý, U. Javornik, Z. Materová, O. Zsiros, P. Šket, J. Plavec, V. Špunda, G. Garab, Lipid-polymorphism of plant thylakoid membranes. Enhanced non-bilayer lipid phases associated with increased membrane permeability, Physiol. Plant. 166 (2019) 278–287, https://doi.org/10.1111/ppl.12929.

[28] S. Santabarbara, F. Villafiorita Monteleone, W. Remelli, F. Rizzo, B. Menin, A.P. Casazza, Comparative excitation-emission dependence of the F V /F M ratio in model green algae and cyanobacterial strains, Physiol. Plant. 166 (2019) 351–364, https://doi.org/10.1111/ppl.12931.

[29] Y.Y. He, D.P. Häder, UV-B-induced formation of reactive oxygen species and oxidative damage of the cyanobacterium *Anabaena* sp.: protective effects of ascorbic acid and N-acetyl-L-cysteine, J. Photochem. Photobiol. B Biol. 66 (2002) 115–124, https://doi.org/10.1016/S1011-1344(02)00231-2.

[30] R.P. Rastogi, S.P. Singh, D.P. Häder, R.P. Sinha, Detection of reactive oxygen species (ROS) by the oxidant-sensing probe 2′,7′-dichlorodihydrofluorescein diacetate in the cyanobacterium *Anabaena variabilis* PCC 7937, Biochem. Biophys. Res. Commun. 397 (2010) 603–607, https://doi.org/10.1016/j.bbrc.2010.06.006.

[31] S.P. Singh, R.P. Rastogi, D.P. Häder, R.P. Sinha, Temporal dynamics of ROS biogenesis under simulated solar radiation in the cyanobacterium *Anabaena variabilis* PCC 7937, Protoplasma. 251 (2014) 1223–1230, https://doi.org/10.1007/s00709-014-0630-3.

[32] S. Neelam, R. Subramanyam, Alteration of photochemistry and protein degradation of photosystem II from *Chlamydomonas reinhardtii* under high salt grown cells, J. Photochem. Photobiol. B Biol. 124 (2013) 63–70, https://doi.org/10.1016/j.jphotobiol.2013.04.007.

[33] A.F. Talebi, M. Tabatabaeit, S.K. Mohtashami, M. Tohidfar, F. Moradi, Comparative salt stress study on intracellular ion concentration in marine and salt-adapted freshwater strains of microalgae, Not. Sci. Biol. 5 (2013) 309–315, https://doi.org/10.15835/nsb539114.

[34] G. Demetriou, C. Neonaki, E. Navakoudis, K. Kotzabasis, Salt stress impact on the molecular structure and function of the photosynthetic apparatus - the protective role of polyamines, Biochim. Biophys. Acta Bioenerg. 1767 (2007) 272–280, https://doi.org/10.1016/j.bbabio.2007.02.020.

[35] Y. Olsen, G. Knutsen, T. Lien, Characteristics of phosphorus limitation in *Chlamydomonas Reinhardth* (*Chlorophyceae*) and its palmelloids, J. Phycol. 19 (1983) 313–319, https://doi.org/10.1111/j.0022-3646.1983.00313.x.

[36] M. Lurling, W. Beekman, Palmelloids formation in *Chlamydomonas reinhardtii*: defence against rotifer predators? Ann. Limnol. 42 (2006) 65–72, https://doi.org/10.1051/limn/2006010.

[37] A.N. Jamers, W.I.M. De Coen, Effect assessment of the herbicide paraquat on a green alga using differential gene expression and biochemical biomarkers, Environ. Toxicol. Chem. 29 (2010) 893–901, https://doi.org/10.1002/etc.102.

[38] D.K. Khona, S.M. Shirolikar, K.K. Gawde, E. Hom, M.A. Deodhar, J.S. D'Souza, Characterization of salt stress-induced palmelloids in the green alga, *Chlamydomonas reinhardtii*, Algal Res. 16 (2016) 434–448, https://doi.org/10.1016/j.algal.2016.03.035.

[39] I. Visviki, D. Santikul, The pH tolerance of *Chlamydomonas applanata* (volvocales, chlorophyta), Arch. Environ. Contam. Toxicol. 38 (2000) 147–151, https://doi.org/10.1007/s002449910018.

[40] R. Kakarla, J.W. Choi, J.H. Yun, B.H. Kim, J. Heo, S. Lee, D.H. Cho, R. Ramanan, H.S. Kim, Application of high-salinity stress for enhancing the lipid productivity of *Chlorella sorokiniana* HS1 in a two-phase process, J. Microbiol. 56 (2018) 56–64, https://doi.org/10.1007/s12275-018-7488-6.

[41] J. Church, J.H. Hwang, K.T. Kim, R. McLean, Y.K. Oh, B. Nam, J.C. Joo, W.H. Lee, Effect of salt type and concentration on the growth and lipid content of *Chlorella vulgaris* in synthetic saline wastewater for biofuel production, Bioresour. Technol. 243 (2017) 147–153, https://doi.org/10.1016/j.biortech.2017.06.081.

[42] W. Fu, G. Paglia, M. Magnúsdóttir, E.A. Steinarsdóttir, S. Gudmundsson, B.T. Palsson, Ó.S. Andrésson, S. Brynjólfsson, Effects of abiotic stressors on lutein production in the green microalga *Dunaliella salina*, Microb. Cell Factories 13 (2014) 1–9, https://doi.org/10.1186/1475-2859-13-3.

[43] M. Wältermann, A. Steinbüchel, Neutral lipid bodies in prokaryotes: recent insights into structure, formation, and relationship to eukaryotic lipid depots, J. Bacteriol. 187 (2005) 3607–3619, https://doi.org/10.1128/JB.187.11.3607-3619.2005.

[44] M. Siaut, S. Cuiné, C. Cagnon, B. Fessler, M. Nguyen, P. Carrier, A. Beyly, F. Beisson, C. Triantaphylidès, Y. Li-Beisson, G. Peltier, Oil accumulation in the model green alga *Chlamydomonas reinhardtii*: characterization, variability between common laboratory strains and relationship with starch reserves, BMC Biotechnol. 11 (2011), https://doi.org/10.1186/1472-6750-11-7.

[45] R. Ünnep, O. Zsiros, K. Solymosi, L. Kovács, P.H. Lambrev, T. Tóth, R. Schweins, D. Posselt, N.K. Székely, L. Rosta, G. Nagy, G. Garab, The ultrastructure and flexibility of thylakoid membranes in leaves and isolated chloroplasts as revealed by small-angle neutron scattering, Biochim. Biophys. Acta Bioenerg. 2014 (1837) 1572–1580, https://doi.org/10.1016/j.bbabio.2014.01.017.

[46] G. Garab, H. van Amerongen, Linear dichroism and circular dichroism in photosynthesis research, Photosynth. Res. 101 (2009) 135–146, https://doi.org/10.1007/s11120-009-9424-4.

[47] G. Garab, Hierarchical organization and structural flexibility of thylakoid membranes, Biochim. Biophys. Acta Bioenerg. 2014 (1837) 481–494, https://doi.org/10.1016/j.bbabio.2013.12.003.

[48] H. Kirchhoff, Chloroplast ultrastructure in plants, New Phytol. 223 (2019) 565–574, https://doi.org/10.1111/nph.15730.

[49] L. Li, E.M. Aro, A.H. Millar, Mechanisms of photodamage and protein turnover in photoinhibition, Trends Plant Sci. 23 (2018) 667–676, https://doi.org/10.1016/j.tplants.2018.05.004.

[50] L. Wolf, T. Cummings, K. Müller, M. Reppke, M. Volkmar, D. Weuster-Botz, Production of β-carotene with *Dunaliella salina* CCAP19/18 at physically simulated outdoor conditions, Eng. Life Sci. 21 (2021) 115–125, https://doi.org/10.1002/elsc.202000044.

[51] R. De Philippis, C. Sili, G. Tassinato, M. Vincenzini, R. Materassi, Effects of growth conditions on exopolysaccharide production by *Cyanospira capsulata*, Bioresour. Technol. 38 (1991) 101–104, https://doi.org/10.1016/0960-8524(91)90138-A.